AGU ADVANCING EARTH AND SPACE SCIENCE

Geophysical Research Letters®

RESEARCH LETTER
10.1029/2021GL094442

Key Points:

- Continental weathering is conventionally considered to be the only phosphorus source to planetary biospheres
- We experimentally demonstrate that weathering of ocean crust under anoxic conditions releases significant amounts of bioavailable phosphorus
- Habitable planets (including the earliest Earth) without subaerial continents may support significant biogenic gas fluxes to the atmosphere

Supporting Information:

Supporting Information may be found in the online version of this article.

Correspondence to:

D. Syverson and C. T. Reinhard,
drew.syverson@yale.edu;
chris.reinhard@eas.gatech.edu

Citation:

Syverson, D. D., Reinhard, C. T., Isson, T. T., Holstege, C. H., Katchinoff, J. A. R., Tutolo, B. M., et al. (2021). Nutrient supply to planetary biospheres from anoxic weathering of mafic oceanic crust. *Geophysical Research Letters*, *48*, e2021GL094442. https://doi.org/10.1029/2021GL094442

Received 24 MAY 2021
Accepted 17 SEP 2021

Nutrient Supply to Planetary Biospheres From Anoxic Weathering of Mafic Oceanic Crust

D. D. Syverson[1], C. T. Reinhard[2,3,4], T. T. Isson[1,5], C. H. Holstege[1], J. A. R. Katchinoff[1], B. M. Tutolo[6], B. Etschmann[7], J. Brugger[7], and N. J. Planavsky[1,3]

[1]Department of Earth and Planetary Sciences, Yale University, New Haven, CT, USA, [2]Georgia Institute of Technology, Earth and Atmospheric Sciences, Atlanta, GA, USA, [3]University of California - Riverside, NASA Interdisciplinary Consortia for Astrobiology Research (ICAR), Alternative Earths Team, Riverside, CA, USA, [4]Georgia Institute of Technology, NASA Nexus for Exoplanet System Science (NExSS), Atlanta, GA, USA, [5]University of Waikato (Tauranga), Faculty of Science and Engineering, Hillcrest, New Zealand, [6]Department of Geosciences, University of Calgary, Calgary, AB, Canada, [7]Earth, Atmosphere and Environment, Monash University, Melbourne, VIC, Australia

Abstract Phosphorus is an essential element for life, and the phosphorous cycle is widely believed to be a key factor limiting the extent of Earth's biosphere and its impact on remotely detectable features of Earth's atmospheric chemistry. Continental weathering is conventionally considered to be the only source of bioavailable phosphorus to the marine biosphere, with submarine hydrothermal processes acting as a phosphorus sink. Here, we use a novel ^{29}Si tracer technique to demonstrate that alteration of submarine basalt under anoxic conditions leads to significant soluble phosphorus release, with an estimated ratio between phosphorus release and CO_2 consumption ($\sum PO_4^{3-}/\sum CO_2$) of 3.99 ± 1.03 μmol mmol^{-1}. This ratio is comparable to that of modern rivers, suggesting that submarine weathering under anoxic conditions is potentially a significant source of bioavailable phosphorus to planetary oceans and that volatile-rich Earth-like planets lacking exposed continents could develop robust biospheres capable of sustaining remotely detectable atmospheric biosignatures.

Plain Language Summary It is conventionally thought that continents above sea level are required in order for habitable planets to support a robust biosphere. We use experimental geochemistry and a simple model of biological cycling to show that this is incorrect, significantly expanding the possible range of planets that may host surface biospheres that would be detectable through telescope observations.

1. Introduction

Phosphorus (P) is a critical component of the genetic and energetic machinery of all life and plays key structural roles in most organisms. Indeed, recent debate has bolstered the case that P is not only essential for life on Earth but is also likely central for recognizable biochemistry more broadly (Erb et al., 2012; Reaves et al., 2012). Recent biogeochemical modeling and reconstructions of the evolution of marine phosphate (PO_4^{3-}) concentrations from Earth's rock record indicate that P has been the ultimate limiting nutrient for the biosphere throughout Earth's history (Derry, 2015; Laakso & Schrag, 2014, 2018), and it has also been argued that P would be expected to limit the extent of life on exoplanets where oxygenic photosynthesis has evolved (Reinhard et al., 2017). Therefore, a mechanistic understanding of how the global P cycle has changed through time is crucial both for a basic understanding of the history of life on our planet and in the development of predictive frameworks for the production and maintenance of exoplanet biosignatures (Meadows et al., 2018).

Marine PO_4^{3-} concentrations are controlled through time by the interplay between the magnitude of P source(s) into the ocean and the efficiency of P burial. Continental weathering, an important long-term CO_2 sink that acts to regulate planetary climate, is also the only significant source of P to the modern oceans (Ruttenberg, 2003). Submarine weathering of basaltic oceanic crust, while also serving as a long-term CO_2 sink, currently acts a significant removal process of P from marine systems (L. A. Coogan & Gillis, 2013; McManus et al., 2019; Wheat et al., 2003, 2017). For example, roughly 20% of the P sourced to the oceans today is removed through seafloor weathering of basalt (Ruttenberg, 2003; Wheat et al., 2003). The remainder is removed in association with the burial of authigenic apatite and carbonate minerals, organic P, and

iron oxides in marine sediments. It has also been proposed that anoxic and iron-rich (ferruginous) oceans, which were widespread on the early Earth (Poulton & Canfield, 2011; Song et al., 2017), lead to enhanced P scavenging through adsorption onto iron oxide minerals formed near the oxygenated ocean-atmosphere interface, through the precipitation of reduced iron-phosphate minerals, such as vivianite, directly from seawater, or through scavenging onto a range of other reduced Fe-bearing mineral phases (Bjerrum & Canfield, 2002; Derry, 2015; Johnson et al., 2020; Reinhard et al., 2017).

Phosphorus removal during seafloor weathering may have been enhanced in Earth's past, given that it is likely that oceanic crust weathering played a more significant role in weathering and CO_2 sequestration prior to the emergence of continents above sea level and the proliferation of land plants in terrestrial ecosystems (Krissansen-Totton et al., 2018; Mills et al., 2014). However, previous work has neglected the possibility that dissolved P may become liberated into seawater during marine weathering of oceanic crust in the absence of dissolved O_2 — as a natural result of limited Fe^{2+} oxidation and subsequent P scavenging. Although mid-ocean ridge basalts (MORB) typically do not contain igneous apatite, P^{5+} substitutes for Si^{4+} in primary silicate minerals (Koritnig, 1965; Watson, 1980), and this P could potentially be released during submarine basalt weathering. If operative, this process would reshape our view of the evolution of the P cycle on Earth (Mills et al., 2014; Reinhard et al., 2017) and would become an important component of attempts to predict planetary P cycling on habitable exoplanets. Here, we provide direct experimental support for the idea that seafloor weathering of oceanic crust under anoxic marine conditions can be a significant source of bioavailable P to aqueous systems, compare our observations with modern seafloor weathering systems, and provide initial estimates of the potential global biogeochemical impacts of this process.

2. Materials and Methods

We use an enriched dissolved $^{29}SiO_2$ tracer to directly and accurately correlate the extent of primary silicate mineral dissolution with the amount of PO_4^{3-} mobilized into seawater upon reaction with natural submarine basalt. We focus here on two sets of experiments, one utilizing fresh submarine basalt and one in which the fresh submarine basalt was treated with the citrate-bicarbonate-dithionite (CBD) reductive dissolution procedure designed to remove pre-existing Fe^{3+}-oxides associated with the partial oxidation during recovery from the seafloor (Mehra & Jackson, 1958) along with associated elements, in particular P, that have a high affinity toward adsorption onto Fe^{3+}-oxides. We combine extensive mineral characterization of the reactant basalt with time-series changes in solution chemistry and thermodynamic modeling to evaluate the efficacy of seafloor weathering of basalt as a potential source of soluble, bioavailable phosphorus under the anoxic conditions characteristic of the early Earth and reducing habitable exoplanets lacking continents above sea level (see Supporting Information S1). Oxygenated basalt weathering experiments were also conducted in order to demonstrate the removal and retention of dissolved PO_4^{3-} as a consequence of the formation of Fe^{3+}-oxide minerals upon reaction, providing a comparative analysis of PO_4^{3-} mobility with the anoxic experiments (see Supporting Information S1).

Reactant basalt was extensively characterized before and after reaction using scanning electron microscopy (SEM), electron microprobe (EMPA) with wavelength-dispersive X-ray spectroscopy (WDS), coupled with synchrotron X-ray fluorescence mapping (SXRF), and Fe K-edge (7.112 keV) X-ray absorption near-edge spectroscopy (XANES) imaging (see Supporting Information S1). Time-series measurements of solution chemistry from experiments were performed using a Thermo Scientific™ Orion™ PerpHecT™ ROSS™ Combination pH Micro Electrode and Thermo Scientific™ Element™ XR inductively coupled plasma mass spectrometer (ICP-MS). The relative standard deviation (2σ) of the ICP-MS measurements ranges between 6% and 10% for P, 1%–5% for Fe, Mn, and Ni, 1%–3% for ^{28}Si, ^{29}Si, and ^{30}Si, and 1%–2% for the major cations, Ca^{2+} and Mg^{2+}. The range in temperatures prescribed for the basalt weathering experiments, 15–75°C, is similar to temperatures associated with modern low-temperature seafloor springs and is within the range estimated through oxygen isotope composition of carbonate minerals formed within altered oceanic crust (Coogan & Gillis, 2013; Coogan et al., 2019; Gillis & Coogan, 2011; Wheat et al., 2017). The Geochemist's Workbench v. 12.0.4 (Bethke et al., 2018), outfitted with a custom database produced using the DBCreate software package (Kong et al., 2013), was used to calculate the speciation of the time-series solution samples.

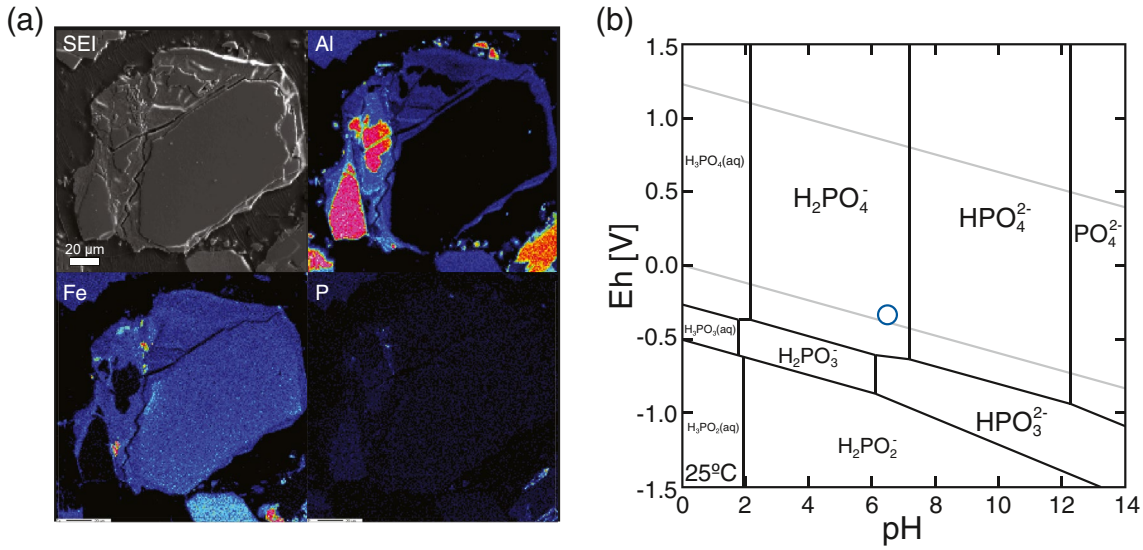

Figure 1. (a) Representative electron microscopy maps of Al, Fe, and P from grains derived from ground basalt sampled from the Juan de Fuca Ridge used in the seafloor weathering experiments. Phosphorus is concentrated along areas of altered grains that are concentrated in Fe, attributable to a mixture of secondary Fe^{3+}-oxide minerals and clays formed upon interaction with seawater at the sampling location. (b) Activity diagram showing the speciation of phosphorus in solution as a function of pH and solution redox state (Eh) at 25°C. The open circle shows the conditions of our seafloor weathering experiments, while the gray lines show the stability limits of water. Hot colors toward red represent high concentrations of the element of interest.

3. Results and Discussion

Mineralogy and element distributions in reactant basalt are shown in Figure 1a and Figures S3 and S4, while detailed time-series solution and CBD extraction chemistry are given in Figure 2, Tables S1–S4 and Figures S6–S11. Analysis by EMPA demonstrates that primary PO_4^{3-} occurs principally as a trace phase within silicates (rather than a more concentrated P-bearing mineral such as apatite), present between 0.01 and 0.4 wt% as P_2O_5 (Figure 1a). Prior to reductive CBD treatment, some P is also concentrated on altered surfaces in association with secondary Fe-oxides and clay mineral phases (Figure 1a), as confirmed by SXRF and XANES imaging (Figure S4). Thermodynamic analysis suggests that the soluble P produced under our experimental conditions is present exclusively as P^{5+} (Figure 1b), consistent with release of trace substituted P in the silicate lattice during basalt dissolution into a protonated PO_4^{3-} pool (predominantly $H_2PO_4^-$). These observations, together with results from the oxygenated experiments, indicate that the lack

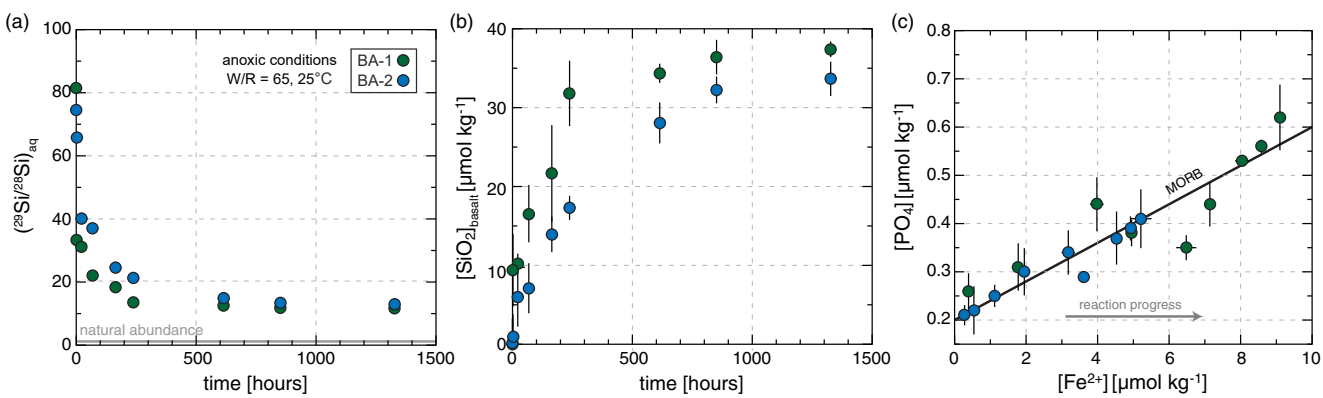

Figure 2. Time-series solution chemistry for the anoxic seafloor weathering experiments (BA-1 and BA-2). (a) Dissolved $^{29}Si/^{28}Si$ ratio of experimental solutions, showing a rapid drop accompanying the dilution of $^{29}SiO_2$-enriched synthetic seawater by dissolved Si derived from basalt dissolution with a natural abundance $^{29}Si/^{28}Si$ ratio. (b) Calculated dissolved SiO_2 derived from dissolution of basalt. (c) Dissolved Fe^{2+} and PO_4^{3-} concentrations in experimental solutions, showing progressive increase in both species with continued reaction progress. Black line in (c) shows the P/Fe ratio expected for dissolution of fresh mid-ocean ridge basalt (MORB).

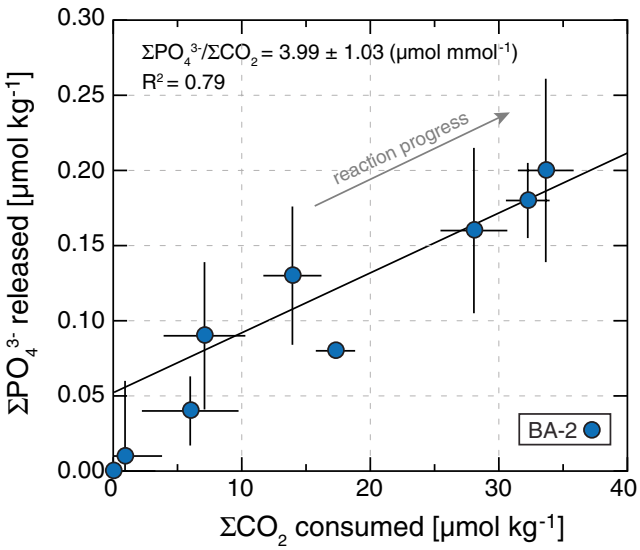

Figure 3. Relationship between the amount of PO_4^{3-} released into reactant seawater and the predicted CO_2 consumed in experiment BA-2 (including reductive dissolution pre-treatment) upon reaction with basalt under anoxic conditions determined from the time-series $^{29}Si/^{28}Si$ data. Solid line shows linear least squares regression of the time-series data, the slope of which yields our estimated mobility ratio ($\Sigma PO_4^{3-}/\Sigma CO_2$) for submarine basalt weathering under anoxic conditions, 3.99 ± 1.03 (μmol $mmol^{-1}$) (±1σ). The experiment, BA-2, was used for this analysis since it had undergone the citrate-bicarbonate-dithionite (CBD) reductive dissolution pretreatment to specifically remove any pre-existing Fe^{3+}-oxide minerals associated with the natural basalt recovered from the seafloor that are enriched in PO_4^{3-} and trace metals.

of Fe-oxide precipitation during seafloor weathering of basalt under anoxic conditions leads to efficient release of soluble reactive P into percolating fluids during silicate dissolution.

Time-series solution chemistry also provide strong evidence for effective mobilization of bioavailable P during basalt dissolution under anoxic conditions (Figures 2, S6 and S8). The rapid decrease in the bulk $^{29}Si/^{28}Si$ ratio of the experimental seawater solutions, together with the roughly constant total dissolved SiO_2 concentrations, reflects the dissolution of reactant basalt, mixing of isotopically natural SiO_2 with $^{29}SiO_2$-enriched synthetic seawater, and precipitation of Si-bearing secondary minerals (Tables S1 and S4, Figure 2a). Our tracer results, which allow us to estimate the contribution of basalt-derived dissolved Si to the overall SiO_2 budget of the system (see Supporting Information S1), demonstrate a sharp increase in basalt-derived aqueous Si with reaction progress, asymptotically reaching concentrations of ~35 μmol kg^{-1} after ~1,300 hr (Figure 2b). As silicate dissolution progresses, we observe significant mobility of both dissolved Fe^{2+} and PO_4^{3-} with continued reaction progress (Figure 2c). These results are in stark contrast to the oxygenated basalt weathering experiments, in which dissolved Fe derived from the dissolution of primary silicate minerals remained below the detection limit while P was either removed from solution (despite high initial dissolved P levels) or remained at steady state levels throughout reaction progress as a consequence of adsorption onto pre-existing and incipiently formed Fe^{3+}-oxide minerals (see Table S2 and Figure S7).

We can further evaluate the potential of submarine basalt weathering under anoxic conditions to serve as a source of bioavailable PO_4^{3-} to the deep ocean by using the time-series $^{29}Si/^{28}Si$ data to quantify the total amount of atmospheric CO_2 that would be consumed upon alteration of primary basalt by seawater. We assume a SiO_2/Alkalinity ratio (Si/Alk) indicative of the composition of tholeiitic basalt, represented here for simplicity as enstatite (e.g., with Si/Alk = 1.0):

$$MgSiO_3 + CO_2 \rightarrow MgCO_3 + SiO_{2(aq)} \quad (1)$$

By combining the time-series changes in $^{29}Si/^{28}Si$ with the total dissolved SiO_2 of the experimental solution, we can use mass balance to quantify the total CO_2 consumed throughout the reaction progress (ΣCO_2). We can then compare ΣCO_2 with the total PO_4^{3-} released during basalt dissolution (ΣPO_4^{3-}), which yields the "mobility ratio" of bioavailable P released per mol of CO_2 consumed during anoxic submarine basalt weathering ($\Sigma PO_4^{3-}/\Sigma CO_2$; Figure 3).

The experiment including the CBD reductive dissolution pretreatment provides the most precise estimate of the $\Sigma PO_4^{3-}/\Sigma CO_2$ ratio during submarine basalt weathering under anoxic conditions, yielding a $\Sigma PO_4^{3-}/\Sigma CO_2$ value of 3.99 ± 1.03 μmol $mmol^{-1}$ (Figure 3). Combining estimated ranges for modern CO_2 outgassing fluxes and riverine PO_4^{3-} fluxes of 5–20 TmolC y^{-1} (Coogan & Gillis, 2020; Isson et al., 2018; Wallmann & Aloisi, 2012) and 0.032–0.058 TmolP y^{-1} (Ruttenberg, 2014), respectively, and stochastically resampling 10^6 times from uniform priors yields a median estimated mobility ratio for the modern Earth system of 3.6 μmol $mmol^{-1}$ with a 95% credible interval of 2.26–6.95 μmol $mmol^{-1}$ (Figure 4a). Our experimental results thus indicate that the $\Sigma PO_4^{3-}/\Sigma CO_2$ value characteristic of submarine basalt weathering under anoxic conditions is of similar magnitude to that estimated for modern weathering of the continental crust (Figure 4a). This suggests that submarine basalt weathering under anoxic conditions off-axis of the mid-ocean ridge (MOR) should in many cases be roughly similar in its effectiveness at exporting bioavailable P during CO_2 consumption as the weathering of continental crust above sea level. Further, these experimental results suggest that PO_4^{3-} may be sourced to the biosphere under anoxic seawater conditions from ridge-flank and on-axis MOR hydrothermal systems, in contrast to modern MOR systems, which

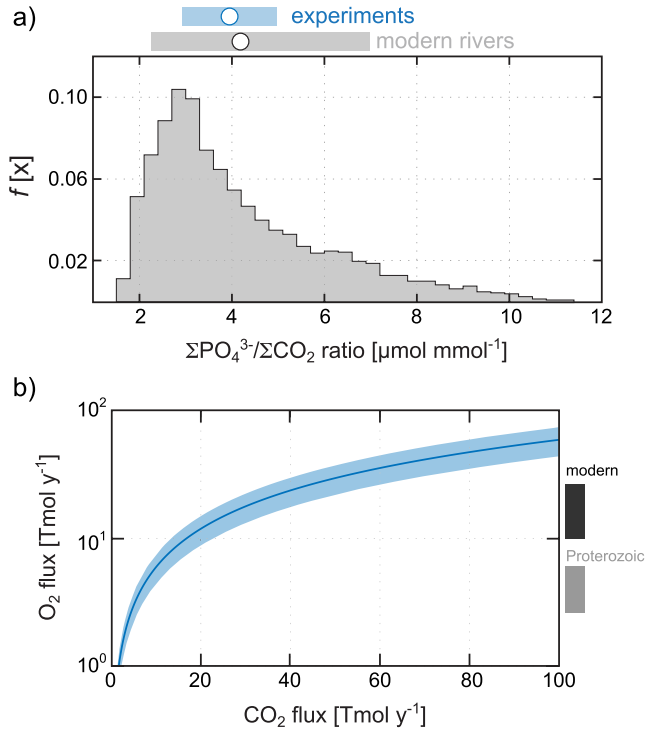

Figure 4. Global biogeochemical impacts of submarine basalt weathering under anoxic conditions. (a) Comparison of mobility ratios ($\Sigma PO_4^{3-}/\Sigma CO_2$) between our experimental results and the modern Earth system, which is dominated by terrestrial weathering of exposed continental landmasses. Gray histogram shows the frequency distribution of resampled estimates for the modern Earth system (see text), with the open circle and shaded bar showing the mean and 95% confidence interval, while the blue circle and shaded bar show the results from our anoxic experiments ($\pm 1\sigma$). (b) Estimated biospheric O_2 flux as a function of volcanic CO_2 input, leading to submarine basalt weathering, P release, and subsequent organic C burial. Calculations assume a P scavenging efficiency of 50% and a global burial C/P ratio of 300 (see text). Blue line and shaded envelope are for the range of mobility ratios shown in (a). Ranges for modern and Proterozoic biospheric O_2 fluxes are given at right (Catling & Kasting, 2017; Ozaki et al., 2019).

demonstrate significant scavenging of dissolved PO_4^{3-} onto Fe^{3+}-oxide minerals formed during seawater-rock interaction and hydrothermal plume formation (Wheat et al., 1996, 2003).

The $\Sigma PO_4^{3-}/\Sigma CO_2$ value obtained by our experiments can be used to illustrate the potential importance of submarine basalt weathering under anoxic conditions for a hypothetical water-rich silicate planet on which seafloor weathering of basalt is the primary CO_2 sink (Abbot et al., 2012; Kite & Ford, 2018). We envision this scenario as being applicable to portions of Earth's earliest history and to Earth-like volatile-rich exoplanet "waterworlds" on which oxygenic photosynthesis has evolved. Conceptually, PO_4^{3-} is released to the ocean as volcanic/metamorphic CO_2 is consumed during submarine basalt weathering, and some fraction of this bioavailable P passes through the biosphere while the remainder is scavenged. This in turn leads to organic C burial and a release of O_2 to the ocean-atmosphere system. The rate of O_2 release associated with this process (J_{O_2}) is given by:

$$J_{O_2} = J_{volc} \cdot f_{weath} \cdot \left[\Sigma PO_4/\Sigma CO_2\right] \cdot \left(1 - \mathcal{E}_P\right) \cdot r_{CP} \quad (2)$$

where J_{volc} represents the rate of volcanic CO_2 outgassing, f_{weath} represents the fraction of CO_2 removal that is balanced by seafloor basalt alteration, ε_P represents a global scavenging efficiency, r_{CP} gives the global net C/P ratio for material buried from the oceans, and $\Sigma PO_4/\Sigma CO_2$ is the mobility ratio as described above. We note that for planets in which the inorganic carbon cycle is balanced by seafloor weathering, the set point of the silicate weathering thermostat (e.g., steady state atmospheric CO_2) will ultimately balance rates of volcanic CO_2 outgassing regardless of the available area of reactive seafloor. For example, if available reactive surface area is small, atmospheric CO_2 will rise until the resultant temperature and seawater chemistry are sufficient for seafloor weathering to balance volcanic outgassing. Because the values of many of these parameters are uncertain even for the Earth system, these estimates are meant only to provide a conceptual framework that allows us to broadly illustrate the potential large-scale impacts of anoxic submarine P release.

Our results indicate that fluxes of PO_4^{3-} from oceanic crust weathering can potentially support significant biospheric O_2 release rates (Figure 4b). For example, at a volcanic CO_2 flux of 20 Tmol y^{-1}, a global C/P burial ratio of 300, and a P scavenging efficiency of 50% our mobility ratio results indicate a biospheric O_2 flux of ~10 Tmol y^{-1}. For comparison, the total net biospheric O_2 flux on the modern Earth is on the order of ~10–20 Tmol O_2 y^{-1} (Catling & Kasting, 2017), while biospheric O_2 fluxes during the Proterozoic following the initial oxygenation of Earth's atmosphere have been estimated to be roughly 2–5 Tmol O_2 y^{-1} (Ozaki et al., 2019). Although the precise values of P scavenging efficiency and global burial C/P ratio are not fully known through Earth's history or across a wide range of planetary scenarios, they are likely to operate inversely to one another (e.g., Reinhard at al., 2017), such that our simple estimate, though non-unique, is likely to be broadly representative.

4. Conclusions

Studies of Earth system evolution and conceptual models used to forecast the emergence and maintenance of biosignatures on volatile-rich exoplanets have neglected the differences in hydrothermal P cycling between oxic and anoxic systems, and have instead implicitly invoked conditions under which P is effectively scavenged through adsorption onto Fe^{3+}-oxide minerals formed from the hydration and oxidation of primary silicates in submarine basalt (Korenaga et al., 2017; Unterborn et al., 2018). Our results stand in strong contrast to this prevailing conceptual model, and thus provide impetus to revisit mechanistic

models for Earth's early oxygen cycle (e.g., Mills et al., 2014) and the factors regulating the oxygen cycles of volatile-rich silicate planets more generally. In particular, it will be important for future work to establish the ocean-atmosphere O_2 "threshold" above which oxygenation of the deep oceans attenuates bioavailable P fluxes by initiating widespread Fe^{2+} oxidation within the ocean interior, and the dynamics of P scavenging and global C/P/O_2 stoichiometry across a wider range of planetary boundary conditions. Nevertheless, our results clearly suggest that biospheres sustained entirely by bioavailable P released during submarine basalt weathering under anoxic conditions, including that of the earliest Earth, are potentially capable of generating extremely high biogenic gas fluxes that rival or exceed even those of the modern Earth. Anoxic submarine weathering should thus be considered an important component of the large-scale redox balance of terrestrial planets.

Data Availability Statement

All datasets for this research are included in this study (and its Supporting Information S1). The geochemical speciation database, solution chemistry, and rock characterization data used in the study are also available at Mendeley Data (https://doi.org/10.17632/mdgz8kxpdh.2). The simple P-C-O_2 mass balance model is determined through Equation 2 and parameters explicitly described in the Supporting Information S1.

Acknowledgments
D. D. Syverson was primarily funded through the Flint Postdoctoral Fellowship provided by Yale University. C. T. Reinhard and N. J. Planavsky acknowledge support from the NASA Interdisciplinary Consortia for Astrobiology Research (ICAR) program (Grant 80NSSC19K0461). C. T. Reinhard acknowledges support from the NASA Nexus for Exoplanet System Science (NExSS) and the NASA Exobiology Program (Grant 80NSSC19K0461). The authors acknowledge the Australian Synchrotron (AS) for awarding beamtime to D. D. Syverson, B. Etschmann, J. Brugger (AS-Proposal #13283). The authors also acknowledge the thoughtful reviews by Gabriel Filippelli and Lee Kump and editorial handling by AE Angelicque White.

References

Abbot, D. S., Cowan, N. B., & Ciesla, F. J. (2012). Indication of insensitivity of planetary weathering behavior and habitable zone to surface land fraction. *The Astrophysical Journal*, *756*, 178. https://doi.org/10.1088/0004-637x/756/2/178

Bethke, C. M., Farrell, B., & Yeakel, S. (2018). *The geochemist's Workbench® release 12.0 — reaction modeling guide*.

Bjerrum, C. J., & Canfield, D. E. (2002). Ocean productivity before about 1.9 Gyr ago limited by phosphorus adsorption onto iron oxides. *Nature*, *417*, 159–162. https://doi.org/10.1038/417159a

Catling, D. C., & Kasting, J. F. (2017). *Atmospheric evolution on inhabited and lifeless worlds*.

Coogan, L. A., Daeron, M., & Gillis, K. M. (2019). Seafloor weathering and the oxygen isotope ratio in seawater: Insight from whole-rock $\delta^{18}O$ and carbonate $\delta^{18}O$ and Δ^{47} from the Troodos ophiolite. *Earth and Planetary Science Letters*, *508*, 41–50. https://doi.org/10.1016/j.epsl.2018.12.014

Coogan, L. A., & Gillis, K. M. (2013). Evidence that low-temperature oceanic hydrothermal systems play an important role in the silicate-carbonate weathering cycle and long-term climate regulation. *Geochemistry, Geophysics, Geosystems*, *14*, 1771–1786. https://doi.org/10.1002/ggge.20113

Coogan, L. A., & Gillis, K. M. (2020). The average Phanerozoic CO_2 degassing flux estimated from the O-isotopic composition of seawater. *Earth and Planetary Science Letters*, *536*, 116151. https://doi.org/10.1016/j.epsl.2020.116151

Derry, L. A. (2015). Causes and consequences of mid-proterozoic anoxia. *Geophysical Research Letters*, *42*, 8538–8546. https://doi.org/10.1002/2015gl065333

Erb, T. J., Kiefer, P., Hattendorf, B., Günther, D., & Vorholt, J. A. (2012). GFAJ-1 is an arsenate-resistant phosphate-dependent organism. *Science*, *337*, 467–470. https://doi.org/10.1126/science.1218455

Gillis, K. M., & Coogan, L. A. (2011). Secular variation in carbon uptake into the ocean crust. *Earth and Planetary Science Letters*, *302*, 385–392. https://doi.org/10.1016/j.epsl.2010.12.030

Isson, T. T., Planavsky, N. J., Coogan, L. A., Stewart, E. M., Ague, J. J., Bolton, E. W., et al. (2018). Evolution of the global carbon cycle and climate regulation on Earth. *Global Biogeochemical Cycles*, *34*, e2018GB006061. https://doi.org/10.1029/2018GB006061

Johnson, B. R., Tostevin, R., Gopon, P., Wells, J., Robinson, S. A., & Tosca, N. J. (2020). Phosphorus burial in ferruginous SiO_2-rich Mesoproterozoic sediments. *Geology*, *48*, 92–96. https://doi.org/10.1130/g46824.1

Kite, E. S., & Ford, E. B. (2018). Habitability of exoplanet waterworlds. *The Astrophysical Journal*, *864*, 75–102. https://doi.org/10.3847/1538-4357/aad6e0

Kong, X.-Z., Tutolo, B. M., & Saar, M. O. (2013). DBCreate: A SUPCRT92-based program for producing EQ3/6, TOUGHREACT, and GWB thermodynamic databases at user-defined T and P. *Computers and Geosciences*, *51*, 415–417. https://doi.org/10.1016/j.cageo.2012.08.004

Korenaga, J., Planavsky, N. J., & Evans, D. A. D. (2017). Global water cycle and the coevolution of the Earth's interior and surface environment. *Philosophical Transactions*, *375*. https://doi.org/10.1098/rsta.2015.0393

Koritnig, S. (1965). Geochemistry of phosphorus — I. The replacement of Si4+ by P5+ in rock-forming silicate minerals. *Geochimica et Cosmochimica Acta*, *29*, 361–371. https://doi.org/10.1016/0016-7037(65)90033-5

Krissansen-Totton, J., Arney, G. N., & Catling, D. C. (2018). Constraining the climate and ocean pH of the early Earth with a geological carbon cycle model. *Proceedings of the National Academy of Sciences of the U S A*, *115*, 4105–4110. https://doi.org/10.1073/pnas.1721296115

Laakso, T. A., & Schrag, D. P. (2014). Regulation of atmospheric oxygen during the Proterozoic. *Earth and Planetary Science Letters*, *388*, 81–91. https://doi.org/10.1016/j.epsl.2013.11.049

Laakso, T. A., & Schrag, D. P. (2018). Limitations on Limitation. *Global Biogeochemical Cycles*, *32*, 486–496. https://doi.org/10.1002/2017gb005832

McManus, J., Wheat, C. G., & Bach, W. (2019). Carbon cycling in low temperature hydrothermal systems: The dorado outcrop. *Geochimica et Cosmochimica Acta*, *264*, 1–12. https://doi.org/10.1016/j.gca.2019.08.010

Meadows, V. S., Reinhard, C. T., Arney, G. N., Parenteau, M. N., Schwieterman, E. W., Domagal-Goldman, S. D., et al. (2018). Exoplanet biosignatures: Understanding oxygen as a biosignature in the context of its environment. *Astrobiology*, *18*, 630–662. https://doi.org/10.1089/ast.2017.1727

Mehra, O. P., & Jackson, M. L. (1958). Iron oxide removal from soils and clays by a dithionite-citrate system buffered with sodium bicarbonate. *Clays and Clay Minerals*, *7*, 317–327. https://doi.org/10.1346/ccmn.1958.0070122

Mills, B., Lenton, T. M., & Watson, A. J. (2014). Proterozoic oxygen rise linked to shifting balance between seafloor and terrestrial weathering. *Proceedings of the National Academy of Sciences of the U S A*, *111*, 9073–9078. https://doi.org/10.1073/pnas.1321679111
Ozaki, K., Reinhard, C. T., & Tajika, E. (2019). A sluggish mid-Proterozoic biosphere and it's effect on Earth's redox balance. *Geobiology*, *17*, 3–11. https://doi.org/10.1111/gbi.12317
Poulton, S. W., & Canfield, D. E. (2011). Ferruginous conditions: A dominant feature of the ocean through earth's history. *Elements*, *7*, 107–112. https://doi.org/10.2113/gselements.7.2.107
Reaves, M. L., Sinha, S., Rabinowitz, J. D., Kruglyak, L., & Redfield, R. J. (2012). Absence of detectable arsenate in DNA from arsenate-grown GFAJ-1 cells. *Science*, *337*, 470–473. https://doi.org/10.1126/science.1219861
Reinhard, C. T., Planavsky, N. J., Gill, B. C., Ozaki, K., Robbins, L. J., Lyons, T. W., et al. (2017). Evolution of the global phosphorus cycle. *Nature*, *541*, 386–389. https://doi.org/10.1038/nature20772
Ruttenberg, K. C. (2003). The global phosphorus cycle. *Treatise on Geochemistry*, *8*, 585–643. https://doi.org/10.1016/b0-08-043751-6/08153-6
Ruttenberg, K. C. (2014). The global phosphorus cycle. In H. D. Holland, & K. K. Turekian (Eds.), *Treatise on geochemistry* (2nd ed., pp. 499–558). Elsevier. https://doi.org/10.1016/b978-0-08-095975-7.00813-5
Song, H., Jiang, H., Poulton, S. W., Wignall, P. B., Tong, J., Song, H., et al. (2017). The onset of widespread marine red beds and the evolution of ferruginous oceans. *Nature Communications*, *8*, 399–406. https://doi.org/10.1038/s41467-017-00502-x
Unterborn, C. T., Desch, S. J., Hinkel, N. R., & Lorenzo, A. (2018). Inward migration of the TRAPPIST-1 planets as inferred from their water-rich compositions. *Nature Astronomy*, *2*, 297–302. https://doi.org/10.1038/s41550-018-0411-6
Wallmann, K., & Aloisi, G. (2012). The global carbon cycle: Geological processes. In A. H. Knoll, D. E. Canfield, & K. O. Konhauser (Eds.), *Fundamentals of geobiology* (pp. 20–35). Blackwell Publishing Ltd. https://doi.org/10.1002/9781118280874.ch3
Watson, B. E. (1980). Apatite and phosphorus in mantle source regions: An experimental study of apatite/melt equilibria at pressures to 25 kbar. *Earth and Planetary Science Letters*, *51*, 322–335. https://doi.org/10.1016/0012-821x(80)90214-9
Wheat, C. G., Feely, R. A., & Mottl, M. J. (1996). Phosphate removal by oceanic hydrothermal processes: An update of the phosphorus budget in the oceans. *Geochimica et Cosmochimica Acta*, *60*, 3593–3608. https://doi.org/10.1016/0016-7037(96)00189-5
Wheat, C. G., Fisher, A. T., McManus, J., Hulme, S. M., & Orcutt, B. N. (2017). Cool seafloor hydrothermal springs reveal global geochemical fluxes. *Earth and Planetary Science Letters*, *476*, 179–188. https://doi.org/10.1016/j.epsl.2017.07.049
Wheat, C. G., McManus, J., Mottl, M. J., & Giambalvo, E. (2003). Oceanic phosphorus imbalance: Magnitude of the mid-ocean ridge flank hydrothermal sink. *Geophysical Research Letters*, *30*, 1895–1899. https://doi.org/10.1029/2003gl017318

References From the Supporting Information

Al-Borno, A., & Tomson, M. B. (1994). The temperature dependence of the solubility product constant of vivianite. *Geochimica et Cosmochimica Acta*, *58*, 5373–5378. https://doi.org/10.1016/0016-7037(94)90236-4
Alt, J. C., & Teagle, D. A. H. (1999). The uptake of carbon during alteration of ocean crust. *Geochimica et Cosmochimica Acta*, *63*, 1527–1535. https://doi.org/10.1016/s0016-7037(99)00123-4
Berner, R. A. (1973). Phosphate removal from sea water by adsorption on volcanogenic ferric oxides. *Earth and Planetary Science Letters*, *18*, 77–86. https://doi.org/10.1016/0012-821x(73)90037-x
Brady, P. V., & Gislason, S. R. (1997). Seafloor weathering controls on atmospheric CO_2 and global climate. *Geochimica et Cosmochimica Acta*, *61*, 965–973. https://doi.org/10.1016/s0016-7037(96)00385-7
Brantley, S. L., & Mellott, N. P. (2000). Surface area and porosity of primary silicate minerals. *American Mineralogist*, *85*, 1767–1783. https://doi.org/10.2138/am-2000-11-1220
Chemtob, S. M., Rossman, G. R., Young, E. D., Ziegler, K., Moynier, F., Eiler, J. M., & Hurowitz, J. A. (2015). Silicon isotope systematics of acidic weathering of fresh basalt, Kilauea Volcano, Hawaii. *Geochimica et Cosmochimica Acta*, *169*, 63–81. https://doi.org/10.1016/j.gca.2015.07.026
Coogan, L. A., & Dosso, S. E. (2015). Alteration of ocean crust provides a strong temperature dependent feedback on the geological carbon cycle and is a primary driver of the Sr-isotopic composition of seawater. *Earth and Planetary Science Letters*, *415*, 38–46. https://doi.org/10.1016/j.epsl.2015.01.027
Coogan, L. A., Gillis, K. M., Pope, M., & Spencer, J. (2017). The role of low-temperature (off-axis) alteration of the oceanic crust in the global Li-cycle: Insights from the Troodos ophiolite. *Geochimica et Cosmochimica Acta*, *203*, 201–215. https://doi.org/10.1016/j.gca.2017.01.002
Etschmann, B. E., Brugger, J., Howard, D., de Jonge, M., Paterson, D., Naidu, R., et al. (2014). Speciation mapping of environmental samples using XANES imaging. *Environmental Chemistry*, *11*, 341–350. https://doi.org/10.1071/en13189
Fisher, L. A., Fougerouse, D., Cleverley, J. S., Ryan, C. G., Micklethwaite, S., Halfpenny, A., et al. (2015). Quantified, multi-scale X-ray fluorescence element mapping using the Maia detector array: Application to mineral deposit studies. *Mineralium Deposita*, *50*, 665–674. https://doi.org/10.1007/s00126-014-0562-z
Frierdich, A. J., Luo, Y., & Catalano, J. G. (2011). Trace element cycling through iron oxide minerals during redox-driven dynamic recrystallization. *Geology*, *39*, 1083–1086. https://doi.org/10.1130/g32330.1
Frierdich, A. J., Scherer, M. M., Bachman, J. E., Engelhard, M. H., Rapponotti, B. W., & Catalano, J. G. (2012). Inhibition of trace element release during Fe(II)-activated recrystallization of Al-, Cr-, and Sn-substituted goethite and hematite. *Environmental Science and Technology*, *46*, 10031–10039. https://doi.org/10.1021/es302137d
Gale, A., Dalton, C. A., Langmuir, C. H., Su, Y., & Schilling, J.-G. (2013). The mean composition of ocean ridge basalts. *Geochemistry, Geophysics, Geosystems*, *14*, 489–518. https://doi.org/10.1029/2012gc004334
Gruber, C., Harpaz, L., Zhu, C., Bullen, T. D., & Ganor, J. (2013). A new approach for measuring dissolution rates of silicate minerals by using silicon isotopes. *Geochimica et Cosmochimica Acta*, *104*, 261–280. https://doi.org/10.1016/j.gca.2012.11.022
Halevy, I., & Bachan, A. (2017). The geologic history of seawater pH. *Science*, *355*, 1069–1071. https://doi.org/10.1126/science.aal4151
Iuliano, M., Ciavatta, L., & De Tommaso, G. (2007). On the solubility constant of strengite. *Soil Science Society of America Journal*, *71*, 1137–1140. https://doi.org/10.2136/sssaj2006.0109
Li, K., Etschmann, B. E., Rae, N., Reith, F., Ryan, C. G., Kirkham, D. H., et al. (2016). Ore petrography using megapixel X-ray imaging: Rapid insights into element distribution and mobilization in complex Pt and U-Ge-Cu ores. *Economic Geology*, *111*, 487–501. https://doi.org/10.2113/econgeo.111.2.487
Liu, Z., Rimstidt, J. D., Zhang, Y., Yuan, H., & Zhu, C. (2016). A stable isotope doping method to test the range of applicability of detailed balance. *Geochemical Perspective Letters*, *2*, 78–86. https://doi.org/10.7185/geochemlet.1608

Mottl, M. J., & Wheat, C. G. (1994). Hydrothermal circulation through mid-ocean ridge flanks: Fluxes of heat and magnesium. *Geochimica et Cosmochimica Acta*, *58*, 2225–2237. https://doi.org/10.1016/0016-7037(94)90007-8

Nicholson, K., & Eley, M. (1997). Geochemistry of manganese oxides: Metal adsorption in freshwater and marine environments. *Geological Society Special Publication*, *119*, 309–326. https://doi.org/10.1144/gsl.sp.1997.119.01.20

Nilsson, N., Lovgren, L., & Sjoberg, S. (1992). Phosphate complexation at the surface of goethite. *Chemical Speciation and Bioavailability*, *4*, 121–130. https://doi.org/10.1080/09542299.1992.11083190

Ravel, B., & Newville, M. (2005). ATHENA, ARTEMIS, HEPHAESTUS: Data analysis for X-ray absorption spectroscopy using IFEFFIT. *Journal of Synchrotron Radiation*, *12*, 537–541. https://doi.org/10.1107/s0909049505012719

Seyfried, W. E. (1977). *Seawater-basalt interaction from 25–300°C and 1500 bars: Implications for the origin of submarine metal-bearing hydrothermal solutions and regulation of ocean chemistry* (pp. 275–500). University of Southern California.

Seyfried, W. E., & Bischoff, J. L. (1979). Low temperature basalt alteration by seawater: An experimental study at 70 and 150°C. *Geochimica et Cosmochimica Acta*, *43*, 1937–1947. https://doi.org/10.1016/0016-7037(79)90006-1

Shock, E. L., Sassani, D. C., Willis, M., & Sverjensky, D. A. (1997). Inorganic species in geologic fluids: Correlations among standard molal thermodynamic properties of aqueous ions and hydroxide complexes. *Geochimica et Cosmochimica Acta*, *61*, 907–950. https://doi.org/10.1016/s0016-7037(96)00339-0

Siever, R. (1992). The silica cycle in the Precambrian. *Geochimica et Cosmochimica Acta*, *56*, 3265–3272. https://doi.org/10.1016/0016-7037(92)90303-z

Sigg, L., & Stumm, W. (1980). The interaction of anions and weak acids with the hydrous goethite (α-FeOOH) surface. *Colloids and Surfaces*, *2*, 101–117.

Staudigel, H., & Hart, S. R. (1983). Alteration of basaltic glass: Mechanisms and significance for the oceanic crust-seawater budget. *Geochimica et Cosmochimica Acta*, *47*, 337–350. https://doi.org/10.1016/0016-7037(83)90257-0

Staudigel, H., Hart, S. R., Schmincke, H. U., & Smith, B. M. (1989). Cretaceous ocean crust at DSDP Sites 417 and 418: Carbon uptake from weathering versus loss by magmatic outgassing. *Geochimica et Cosmochimica Acta*, *53*, 3091–3094. https://doi.org/10.1016/0016-7037(89)90189-0

Stumm, W., Kummert, R., & Sigg, L. (1980). A ligand exchange model for the adsorption of inorganic and organic ligands at hydrous oxide interfaces. *Croatica Chemica Acta*, *53*, 291–312.

Thompson, G. (1973). A geochemical study of the low-temperature interaction of seawater and oceanic igneous rock. *Transactions — American Geophysical Union*, *54*, 1015–1019.

Thompson, G., & Humphris, S. E. (1977). Sewater-rock interactions in the oceanic basement. In *Proceedings of the second international symposium on water-rock interaction*.